JOURNAL OF SOLID STATE CHEMISTRY 106, 330–338 (1993)

Additional Oxygen Ordering in "$La_2NiO_{4.25}$" ($La_8Ni_4O_{17}$). II. Structural Features

A. DEMOURGUES, F. WEILL, B. DARRIET, A. WATTIAUX, J. C. GRENIER, P. GRAVEREAU, AND M. POUCHARD

Laboratoire de Chimie du Solide du CNRS, Université de Bordeaux I, 351, Cours de la Libération, 33405 Talence Cedex, France

Received January 11, 1993; in revised form March 25, 1993; accepted March 29, 1993

On the basis of data obtained from the refinement of neutron diffraction experiments, the structural features of $La_8Ni_4O_{17}$ ("$LaNiO_{4.25}$") are discussed. It is shown that the additional oxygen atoms in the La_2O_2 layers form (O_3^{5-}) polyoxides including one delocalized hole. In the NiO_2 planes, a periodic modulation of the equatorial Ni–O distances characterizes various electronic configurations of the nickel cations and a 2D charge density wave occurs, which is more pronounced at low temperature than at room temperature. A strong coupling between the (O_3^{5-}) polyoxides and the NiO_2 planes results from charge transfer mechanisms, which also account for the stabilization of monovalent nickel (Ni^+) in this compound. The formation of —Ni^+–(O_3^{5-})–Ni^+–(O_3^{5-})— chains along given $(111)_T$ directions is correlated to the interstitial oxygen ordering previously evidenced.

Introduction

The layered perovskite-related materials $La_2NiO_{4+\delta}$, whose structure is closely related to that of the high T_c superconductor $La_2CuO_{4+\delta}$, have been extensively studied; more particularly, special attention has been paid to the accommodation of interstitial oxygen atoms in the lattice in correlation with their physical properties (*1–7*).

An overoxidized material, $La_2NiO_{4+\delta}$, exhibiting a large interstitial oxygen amount with regard to the basic K_2NiF_4-type structure, has recently been prepared using an electrochemical process (*8*). Structural data for the $\delta = 0.25$ composition have been reported in Part I. A monoclinic cell (C-centered; $a = 13.83$ Å, $b = 10.93$ Å, $c = 10.51$ Å, $\beta = 113°30'$), four times bigger than the usual orthorhombic unit cell, has been determined by electron diffraction microscopy (*9*). The structure of this compound has been refined from neutron diffraction data at 300 K and at 9 K. Due to the reflection conditions, three space groups (*C*2, *Cm*, and *C*2/*m*) have been considered. On account of the obtained Rietveld refinement profile (*R*-factors and the Hamilton test) and of calculations of the Madelung energy and site potentials, the *C*2 space group seemed finally to be the most relevant one.

The aim of this publication is to discuss these data, more especially the accomodation of the interstitial oxygen defects in the supercell structure, in relation to previous results (*10–11*). Indeed, many controversies still surround the valence of the extra oxygen atoms and the nature of their association with the apical oxygen atoms of the parent lattice. The question remains open whether O_2^{2-} peroxide ions, O_2^- superoxide ions, or other oxygenated species are formed (*12–15*).

Otherwise it is well known that, in non-stoichiometric oxides, from the moment that interactions between defects exist, the formation of short range, then of extended defects occurs with the entropy and energy

0022-4596/93 $5.00

terms competing for dominance. For instance, in $UO_{2.12}$, a long time ago, Willis (*16*), found a short range ordering of the additional oxygen atoms leading to the formation of oxygen clusters. Later, using neutron diffraction, H. Blank and C. Ronchi (*17*) determined the structure of a single crystal of U_4O_9 ("$UO_{2.25}$") composition and showed a long range ordering of clusters of a new type in the UO_2 lattice.

In a similar way, we suggested the formulation $La_8Ni_4O_{17}$ for the $\delta = 0.25$ composition. We describe in this Part II the nature of the oxygen defects and their ordering in the La_2NiO_4 lattice.

In La_2NiO_4, as far as the "$LaNiO_3$" perovskite type layers are concerned, the small size of La^{3+} results in a low value of the so-called tolerance factor

$$t = \frac{r_{La^{3+}} + r_{O^{2-}}}{\sqrt{2}\,(r_{Ni^{2+}} + r_{O^{2-}})}$$

which creates an equatorial compressive stress in the NiO_2 sheet. This destabilizing stress strongly influences numerous structural, chemical, and electronic properties. As previously quoted (*1*, *18*), from a structural point of view, the stress in the (*a*, *b*) plane leads to an alternating tilting of the NiO_6 octahedra along the $[010]_{Bmab}$ direction and a change in the symmetry ($I_{4/mmm}$ toward *Bmab*).

From a chemical point of view, this stress gives rise to an easy oxidation of Ni^{2+} into Ni^{3+} ($r_{Ni^{3+}} < r_{Ni^{2+}}$), and the equatorial compressive stress gradually decreases. This is the reason that the insertion of additional O_I oxygen atoms in the La_2O_2 layers is easily obtained (*3*, *8*, *12*).

Moreover, we think that electron transfers may also relax the structure, more particularly the electron transfer of $\sigma^{*2}_{x^2-y^2}$ antibonding electrons toward $\sigma^{*2}_{z^2}$ states, which can occur in various ways:

—*either as a spin equilibrium (intraatomic* transfer) Ni^{2+} ($^3B_{1g}$, $S = 1$) $\Leftrightarrow$ Ni^{2+} ($^1A_{1g}$, $S = 0$)

—or as a disproportionation or a charge density wave (interatomic transfer)
$2\ Ni^{2+}$ ($^3B_{1g}$) $\Leftrightarrow$ Ni^{3+} ($^2A_{1g}$) + Ni^{+} ($^2B_{1g}$)
(the ground state terms are given for the D_{4h} symmetry).

From the structural data for $La_8Ni_4O_{17}$ reported in Part I, we focus our attention on the correlations between the nature and the ordering of the interstitial defects and the electronic structure of the nickel cations.

Discussion

1. Environment of the Additional Oxygen Atoms

a. T = 9 K

The O_I additional oxygen is surrounded by four lanthanum cations and four O_z apical oxygen anions. From an ionic point of view, the $d(La–O_I)$ distances are shorter than the sum of the ionic radii of the La^{3+} and O^{2-} ions ($d(La–O_I) = 2.38$ Å $<< r(La^{3+}) + r(O^{2-}) = 2.60$ Å (*19*)) and the lanthanum tetrahedron is rather regular ($107° \leq \alpha(La–O_I–La) \leq 114°$ (Fig. 1a)). In contrast, the oxygen tetrahedron is highly distorted ($94° \leq \alpha(O_z–O_I–O_z) \leq 134°$) (Fig. 1b) and the $O_I–O_z$ distances are very different from each other (2.17 Å $\leq d(O_I–O_z) \leq$ 2.61 Å). More especially, the $O_I–O_z(1)$ and $O_I–O_z(3)$ bond lengths are the shortest (Fig. 1b), which leads us to assume the formation of triatomic oxygen clusters ($O_z(1)–O_I–O_z(3)$) whose average oxygen–oxygen distance is 2.21 ± 0.04 Å.

Figure 2 shows the variation of the O–O distance as a function of the bond order for various oxygen species (*20*). The average $O_I–O_z$ distance ($d(O_I–O_z) = 2.21$ Å) seems to correspond to a bond order of $\frac{1}{4}$. Therefore one can conclude that one hole is delocalized on these three oxygen atoms, which would correspond to the formation of an O_3^{5-} polyoxide. Calculations of the Madelung potentials carried out for the oxygen sites (O_{xy}, $O_z(i)$, O_I) are reported in Table I. Provided that a hole occurs on oxygen atoms, it

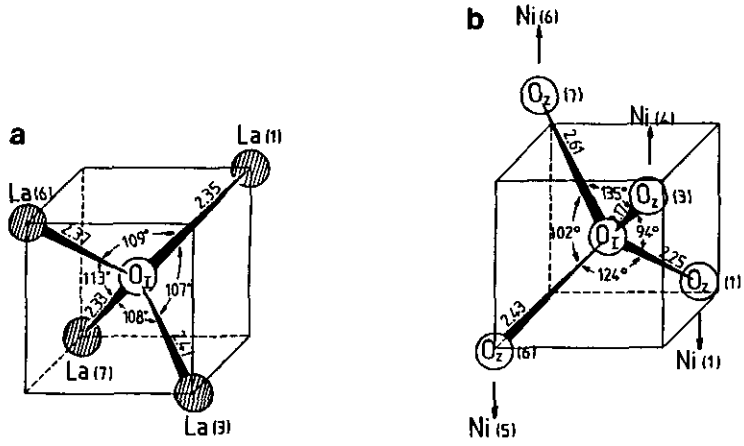

FIG. 1. (a) Representation of the O_ILa_4 tetrahedron at $T = 9$ K. (b) Representation of the $O_IO_{(z)4}$ tetrahedron at $T = 9$ K.

should be located on the atoms for which the Madelung potential is the lowest; i.e., O_I, $O_z(1)$, or $O_z(3)$.

This calculation corroborates the previous assumption concerned with the formation of O_3^{5-}. In addition, this structural feature seems to demonstrate that the additional O_I oxygen atoms are not inserted into the La_2NiO_4 network in the form of either O_2^- superoxide or O_2^{2-} peroxide species as previously reported (*13–15*).

b. T = 298 K

At room temperature, the additional oxygen environment is slightly different from that observed at low temperature. The (O_ILa_4) polyhedron is quite similar ($\bar{d}(O_I\text{–}La) = 2.38$ Å, $04° \leq \alpha(La\text{–}O_I\text{–}La) \leq 114°$). But some $O_I\text{–}O_z(i)$ distances have changed with temperature. The $O_I\text{–}O_z(3)$ bondlength remains unchanged, whereas $d(O_I\text{–}O_z(6))$ slightly decreases. On the other hand, the $O_I\text{–}O_z(7)$ distance decreases all the more as the $O_I\text{–}O_z(1)$ one increases ($\Delta_d \approx 0.13$ Å). Again a triatomic cluster O_3^{5-} is formed but the concerned atoms are different ($O_z(3)\text{–}O_I\text{–}O_z(6)$), $\bar{d}(O_I\text{–}O_z) = 2.23$ Å), Fig. 3).

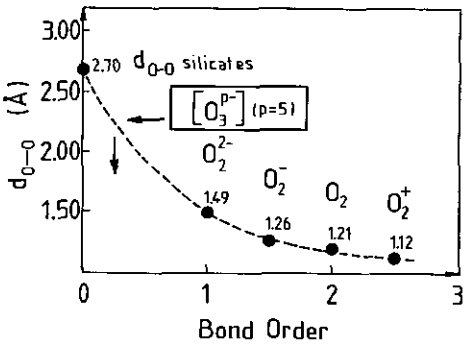

FIG. 2. Variation of the O–O distance as a function of the bond order for various O_2^{n+} species.

TABLE I

MADELUNG POTENTIALS (V) OF THE O_{xy}, $O_z(i)$, AND O_I SITES IN $La_8Ni_4O_{17}$ ($T = 9$ K).

Site	Madelung (V) potentials
O_{xy}	22.98
O_z (1)	13.48
O_z (2)	23.93
O_z (3)	17.80
O_z (4)	22.08
O_z (5)	20.75
O_z (6)	19.10
O_z (7)	17.98
O_z (8)	19.87
O_I	13.25

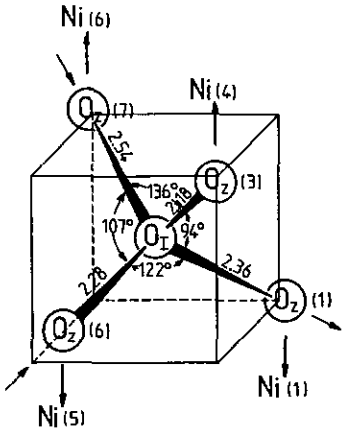

FIG. 3. Representation of the $O_IO_{(z)4}$ tetrahedron at $T = 298$ K.

c. *Comparison with the Oxygen Ionic Complex in U_4O_9 ("$UO_{2.25}$")*

It should be emphasized that similar O–O bondlengths have been determined by Blank and Ronchi (*17*) using neutron diffraction data obtained for U_4O_9 single crystals. In this superstructure of UO_2 these authors assumed the occurrence of an "oxygen ionic complex" (1.96 Å ≤ d(O–O) ≤ 2.37 Å). However, the basic difference between this cluster and the O_3^{5-} polyoxide previously quoted is the location of the additional oxygen atom near the body center of the fluorite-type structure for the former and in the tetrahedral site of the rocksalt-type structure for the latter (Fig. 4).

2. The NiO_6 Octrahedra

Using the *C*2 monoclinic space group for the Rietveld structure refinement of $La_8Ni_4O_{17}$ implies the existence of six different sets of nickel sites in the structure, whereas only one site is available with the *Fmmm* orthorhombic space group. Therefore, the $\sigma^*_{x^2-y^2}$ and $\sigma^*_{z^2}$ bands should be split into narrower bands with energy levels depending on the crystal field stabilization energy and the intraatomic repulsion energy (Hubbard energy). One can therefore assume that nickel cations have various electronic configurations.

Starting from the results of the Rietveld structure refinement at 9 and 298 K (see Part I), the values of the Ni–O distances are reported in Table II. The $d^{\perp}_{(Ni-O)}$ and $d^{\parallel}_{(Ni-O)}$ distances correspond to the directions perpendicular and parallel to the *c*-axis of the basic *I*4/*mmm* tetragonal unit cell, respectively. The $\bar{d}_{(Ni-O)}$ average distances and the θ distortion parameters were calculated according to

$$\bar{d}_{(Ni-O)} = (\tfrac{2}{3} d^{\perp}_{(Ni-O)} + \tfrac{1}{3} d^{\parallel}_{(Ni-O)}),$$

$$\theta = d^{\parallel}_{(Ni-O)}/d^{\perp}_{(Ni-O)}.$$

The value of the θ parameter remains rather high ($\theta \approx 1.15$), which implies that the NiO_6 octahedra are always elongated.

It should also be pointed out that 25% of the nickel cations (Ni(1) and Ni(4)) are affected by two O_I additional oxygen atoms, 50% (Ni(5) and Ni(6)) are affected by only one O_I atom, and 25% (Ni(2) and Ni(3)) are nonaffected.

On the basis of the Ni–O distances and of previous works, we assign probable valence

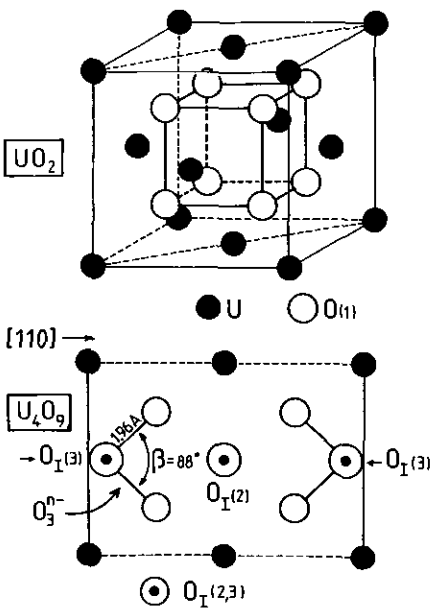

FIG. 4. Structure of U_4O_9 showing the location of the interstitial oxygen atoms.

TABLE II

$d^{\parallel}_{NiO}$, $d^{\perp}_{NiO}$, AND $\bar{d}_{NiO}$ DISTANCES IN THE NiO_6 OCTAHEDRA (THE RATIO $\theta = d^{\parallel}_{NiO}/d^{\perp}_{NiO}$ IS ALSO REPORTED)

Ni	Number of equivalents	$d^{\parallel}_{NiO}$	$d^{\perp}_{NiO}$	$\bar{d}_{NiO}$	θ	$d^{\parallel}_{NiO}$	$d^{\perp}_{NiO}$	$\bar{d}_{NiO}$	θ
(1)	2	2.27	1.99	2.08	1.14	2.20	1.94	2.03	1.13
(2)	2	2.20	1.89	1.99	1.16	2.21	1.90	2.00	1.16
(3)	2	2.23	1.90	2.01	1.17	2.20	1.90	2.00	1.16
(4)	2	2.23	1.98	2.06	1.13	2.26	1.98	2.07	1.14
(5)	4	2.17	1.94	2.01	1.12	2.20	1.94	2.02	1.13
(6)	4	2.21	1.92	2.01	1.15	2.22	1.95	2.04	1.14

states to the various nickel cations at T = 9 K and at room temperature.

a. T = 9 K

At first, it is important to note that the Ni(1) and Ni(4) sites have the largest size, even larger than that of the Ni^{2+} polyhedron in the $La_2NiO_{4.00}$ compound ($d^{\perp}_{(Ni-O)}$ = 1.943 Å, $d^{\parallel}_{(Ni-O)}$ = 2.264 Å).

In an earlier work, Crespin *et al.* prepared the pure monovalent nickel oxide $LaNiO_2$ (*21*) for which the nickel environment is a square planar coordination. Using X-ray diffraction and EXAFS, they determined the distance $d_{(Ni-O)}$ = 1.985 Å. Similar results were recently obtained for the mixed valence Ni^{+}/Ni^{2+} nickelate $Nd_4Ni_3O_8$ ($d_{(Ni-O)}$ = 1.96 Å (*22*)).

On the other hand, we recently reported a large anisotropic EPR signal (ΔH = 550 G, $g^{\parallel} = 2.33 > g^{\perp} = 2.03$ (*8*)), which was assigned either to Ni^{3+} in a flattened octahedral site ($t^6_{2g}\, d^1_{x^2-y^2}$) or to Ni^{+} in a stretched octahedral site ($t^6_{2g} d^2_{z^2} d^1_{x^2-y^2}$). On account of the θ parameter ($\theta >> 1$), one can conclude that this signal results from the presence of Ni^{+} that is isoelectronic to Cu^{2+}. Therefore the valence of Ni(1) and Ni(4) would be close to +1 ($t^6_{2g} d^2_{z^2} d^1_{x^2-y^2}$).

The valence assignment of the remaining sites appears more difficult but taking into account that the $d^{\perp}_{(Ni-O)}$ distances relative to Ni(2) and Ni(3) are the smallest, the valence of these cations might be close to +3.

From a general viewpoint, the NiO_6 octahedra are always elongated and one can consider two limit electronic configurations of the nickel cations: $t^6_{2g} d^2_{z^2}\ d^1_{x^2-y^2}$ (Ni^{+}) and $t^6_{2g} d^1_{z^2}\ d^0_{x^2-y^2}$ (Ni^{3+}). Intermediate states would correspond to the $t^6_{2g} d^{1+\alpha}_{z^2}\ d^{\beta}_{x^2-y^2}$ electronic configuration, where α and β are lower than 1. Particular values lead for instance to Ni^{2+}(HS) (α = 0, β = 1) or Ni^{2+}(LS) (α = 1, β = 0).

Considering the occurrence of the O_3^{5-} polyoxide and on the basis of the chemical formulation $La_8Ni_4O_{17}$, the average oxidation state of the nickel is +2.25. Since 25% of nickel cations have the +1 valence state (Ni(4) and Ni(5)) and 25% have the +3 valence state (Ni(2), Ni(3)), the remaining electron distribution on nickel cations (Ni(5) and Ni(6)) should correspond to an intermediate valence state of +2.50.

Magnetic susceptibility measurements that will be reported in the near future (*23*) show Curie–Weiss behavior at low temperature. The value of the Curie constant determined in the temperature range (4.2 K $\leq T \leq$ 150 K, $C \approx$ 0.33 emu K/Ni) is lower than the theoretical value corresponding to one unpaired electron (C = 0.375 emu K/Ni), which leads to the conclusion that the Ni^{2+} cations are mainly in the low spin state ($\alpha \approx 1$, $\beta \approx 0$). Similar conclusions were claimed by Takeda *et al.* for the $La_{2-x}Sr_xNiO_4$ system (*24*).

Figure 5a shows the NiO_6 octahedra in the $(100)_m$ plane and the various Ni–O dis-

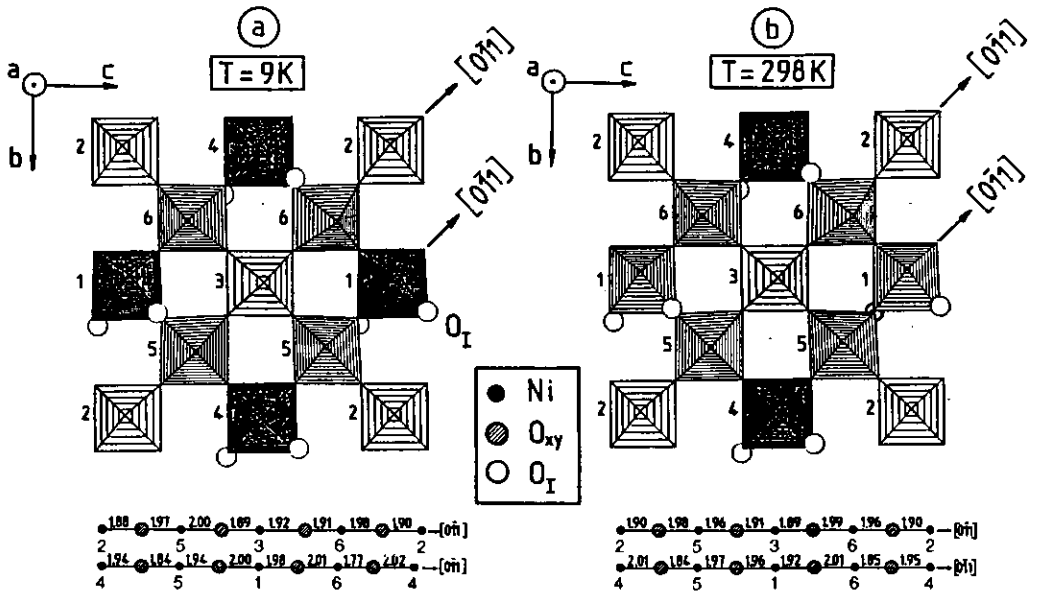

FIG. 5. The modulation of the Ni–O distances in the $(100)_m$ plane at $T = 9$ and 298 K. The electronic density is maximal for the dark octahedra (Ni^+) and minimal for the light ones (Ni^{3+}).

tances. One can note an important variation of these distances along the [011] and [0$\bar{1}$1] directions (1.77 Å $\leq d^{\perp}_{(Ni-O)} \leq$ 2.01 Å).

This modulation and the above description of the electronic configurations of the nickel cations suggest the occurrence of a periodic lattice distortion (PLD), which would be correlated to a two dimensional charge density wave (CDW) or to a modulated disproportionation in the $(100)_m$ plane.

b. T = 298 K

At room temperature the Ni(2) and Ni(3) octrahedra remain unchanged with regard to the low temperature situation. In the same way Ni(4) cations still have the +1 valence state, which is in agreement with the EPR signal observed at room temperature (*8*).

In contrast, according to the Ni–O distances (Table II and Fig. 5b), the electron distribution in the $\sigma^{*}_{z^2}$ and $\sigma^{*}_{x^2-y^2}$ narrow bands of the Ni(1), Ni(5), and Ni(6) cations is changed and seems to imply an electron transfer: Ni(1) → Ni(5) or Ni(6).

As shown in Fig. 5b, although a modulation of the Ni–O distances still exists (1.85 Å $\leq d^{\perp}_{(Ni-O)} \leq$ 2.01 Å), the PLD seems nevertheless to be less pronounced.

3. Electron Transfer between the O_3^{5-} Polyoxides and the NiO_2 Sheets

In this section, we examine the coupling between the NiO_2 layers and the O_3^{5-} polyoxides through the d_{z^2} orbitals of nickel cations in terms of electronic transfer. As reported in Table II and as mentioned above, the nickel environments are different (2, 1, or 0 additional oxygen atoms). Therefore various charge transfer reactions can be depicted.

a. T = 9 K

At low temperature, $Ni^+(1)$ and $Ni^+(4)$ are directly affected by two O_3^{5-} polyoxides and one can observe (Fig. 6) the formation of infinite chains,

$$\ldots\text{-}Ni^+(1)\text{-}O_3^{5-}\text{-}Ni^+(4)\text{-}O_3^{5-}\text{-}Ni^{+(1)}\text{-}\ldots,$$

along the $[102]_m$ direction, which is actually

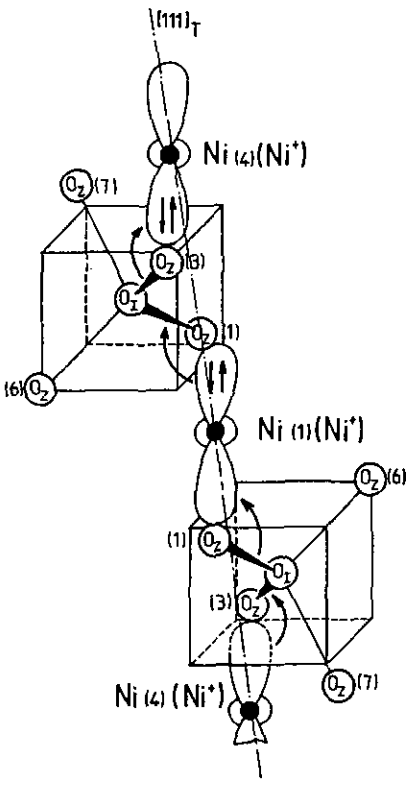

FIG. 6. Electron transfer between the O_3^{5-} polyoxides and the nickel cations along the $[111]_T$ direction in $La_8Ni_4O_{17}$ at $T = 9$ K.

the $[111]_t$ direction of the K_2NiF_4-type unit cell.

The occurrence of a hole on the polyoxide ion and correlatively of Ni^+ should result from the charge transfer equilibrium

$$\underset{d_{z^2}^1 d_{x^2-y^2}^1\,(HS)}{Ni^{2+}} + 3\,O^{2-} \leftrightarrows \underset{d_{z^2}^2 d_{x^2-y^2}^1}{Ni^{+}} + \underset{(2p^5)}{O_3^{5-}}$$

which is strongly shifted towards the right in agreement with our previous conclusions.

This electron transfer is very similar to the equilibrium $M^{n+} + O^{2-} \Leftrightarrow M^{(n-1)+} + O^-$ previously quoted for perovskite related oxides (*25*). Conversely Ni(2) and Ni(3) cations which are the +3 valence state have no additional oxygen atom in their neighborhood, so they cannot be involved in such a charge transfer reaction.

b. T = 298 K

At room temperature the O_3^{5-} polyoxide couples Ni(4) and Ni(5) and one should point out that the infinite chains, previously described at $T = 9$ K, have disappeared (Fig. 7).

In order to explain the electron transfer Ni(1) → Ni(5) or Ni(6) suggested above, two charge transfer equilibria have to be considered,

$$\underset{d_{z^2}^1 d_{x^2-y^2}^1\,(HS)}{Ni^{2+}(1)} + 3\,O^{2-} \underset{(2p^6)}{} \xleftrightarrow{} \underset{d_{z^2}^2 d_{x^2-y^2}^1}{Ni^{+}(1)} + \underset{(2p^5)}{O_3^{5-}} \quad (1)$$

$$\underset{d_{z^2}^2 d_{x^2-y^2}^0\,(LS)}{Ni^{2+}(5)} + \underset{(2p^5)}{O_3^{5-}} \xleftrightarrow{} \underset{d_{z^2}^1 d_{x^2-y^2}^0}{Ni^{3+}(5)} + 3\,O^{2-} \underset{(2p^6)}{}, \quad (2)$$

involving the disproportionation equilibrium in the NiO_2 sheets via the O_3^{5-} polyoxide ion ((1) + (2) → (3)):

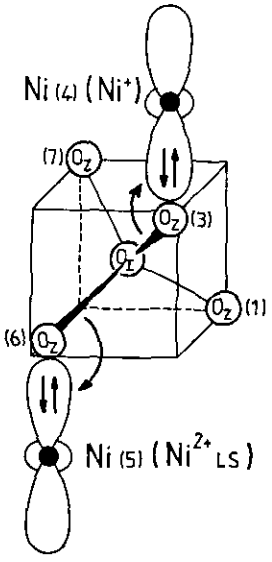

FIG. 7. Electron transfer between the O_3^{5-} polyoxides and the nickel cations in $La_8Ni_4O_{17}$ at $T = 298$ K.

$$Ni^{2+}(1) + Ni^{2+}(5) \leftrightarrows Ni^{+}(1) + Ni^{3+}(5). \quad (3)$$

The last equilibrium, which lies well over on the left, merely explains the electron transfer Ni(1) → Ni(5) or Ni(6) and the fact that the CDW is less pronounced at room temperature than at 9 K (Figs. 5a and b). At $T = 9$ K this equilibrium lies well over on the right.

Conclusion

On the basis of structural data obtained from neutron diffraction experiments on $La_8Ni_4O_{17}$ the following conclusions can be drawn:

—The additional oxygen atoms O_i are intercalated into the "La_2O_2" layers of the La_2NiO_4 lattice in an ordered way along given $\langle 111\rangle_T$ directions of the basic tetragonal unit cell. They occupy sites whose Madelung potential is the lowest compared to other oxygen sites. Because of short distances between them and two neighbor apical atoms, we assume the existence of some bonding character suggesting they form (O_3^{5-}) polyoxides including one delocalized hole.

—In the NiO_2 sheets the periodic modulation of the equatorial Ni–O distances shows, more particularly at low temperature, the presence of a two dimensional charge density wave strongly trapped by the lattice giving rise to a modulated disproportionation $Ni^{(2\pm\lambda)}$ ($0 \leq \lambda \leq 1$). On the basis of the Ni–O bond lengths, oxidation states ranging between +1 and +3 were assigned to the various nickel cations. The unusual monovalent oxidation state of nickel is corroborated by the observed large anisotropic EPR signal. At rising temperature the Ni–O distance modulation is less pronounced (λ decreases).

—a strong correlation between the O_3^{5-} polyoxides of the "$La_2O_{2+\delta}$" layers and the NiO_2 planes exists, which explains why monovalent nickel can be stabilized in this compound. This stabilization results from both

(i) the charge transfer mechanism

$$Ni^{2+}_{(1,4)} + 3\,O^{2-} \Leftrightarrow Ni^{+}_{(1,4)} + O_3^{5-},$$

which is markedly shifted to the left, especially at low temperature,

(ii) and the presence of one hole on the O_3^{5-} polyoxide, which decreases the crystal field along the z axis of the concerned ($Ni^{+}O_6$) octahedra, by decreasing the average negative charge of the ligand and by its small displacement arising from the partially bonding O–O character inside the polyoxide. This coupling also shows the close correlation between the occurrence of a CDW in the NiO_2 planes and the ordering of the additional oxygen atoms into Ni^{+}–O_3^{5+}—Ni^{+}–O_3^{5-} chains along some $\langle 111\rangle_T$ directions as previously depicted in the structural model (*9*).

The formation of such a CDW with a periodic lattice distortion in $La_8Ni_4O_{17}$ results in semiconducting-type behavior, which differs from the metallic-superconducting $La_2CuO_{4+\delta}$ phases for which the electronic configuration of Cu^{2+}, i.e., $3d^9$ and fully occupied dz^2 orbitals, does not allow such a disproportionation.

References

1. K. K. Singh, P. Ganguly, and J. B. Goodenough, *J. Solid State Chem.* **52,** 254 (1984).
2. D. J. Buttrey, J. M. Honig, and C. N. R. Rao, *J. Solid State Chem.* **64,** 287 (1986).
3. D. J. Buttrey, P. Ganguly, J. M. Honig, C. N. R. Rao, R. R. Schartman, and G. N. Subbana, *J. Solid State Chem.* **74,** 233 (1988).
4. Y. Shimokawara and K. Kohn, *Jpn. J. Appl. Phys.* **29**(7), L1124 (1990).
5. T. Freltoft, D. J. Buttrey, G. Aeppli, D. Vaknin, and G. Shirane, *Phys. Rev. B* **44**(10), 5046 (1991).
6. J. Rodriguez-Carvajal, M. T. Fernandez-Diaz, and J. L. Martinez, *J. Phys. Condens. Matter.* **3,** 3215 (1991).
7. K. Yamada, T. Omata, K. Nakajima, S. Hosoya, T. Sumida, and Y. Endoh, *Physica C* **191,** 15 (1992).
8. A. Demourgues, A. Wattiaux, J. C. Grenier, M. Pouchard, J. M. Dance, J. L. Soubeyroux, and P. Hagenmuller, *J. Solid State Chem.*, (in press).

9. A. DEMOURGUES, F. WEILL, J. C. GRENIER, A. WATTIAUX, AND M. POUCHARD, *Physica C* **192,** 425 (1992).
10. A. WATTIAUX, L. FOURNES, A. DEMOURGUES, N. BERNABEN, J-C. GRENIER, AND M. POUCHARD, *Solid State Commun.* **77,** 489 (1991).
11. Z. HIROÏ, T. OBATA, M. TAKANO, AND Y. BANDO, *Phys. Rev. B* **41**(6), 11665 (1990).
12. J. D. JORGENSEN, B. DABROWSKI, S. PEI, D. R. RICHARDS, AND D. G. HINKS, *Phys. Rev. B* **40,** 2187 (1989).
13. C. CHAILLOUT, J. CHENAVAS, S. W. CHEONG, Z. FISK, M. MAREZIO, B. MOROSIN, AND J. E. SCHIRBER, *Physica C* **170,** 87 (1990).
14. M. STRONGIN, S. L. QIN, J. CHEN, C. L. LIN, AND E. M. MCCARRON, *Phys. Rev. B* **41** (10), 7238 (1990).
15. A. BIANCONI, A. CONGIU-CASTALLANO, M. DE SANTIS, P. DELAGU, A. GARGANO, AND R. GIORDI, *Solid State Commun.* **63,** 1135 (1987).
16. B. T. M. WILLIS, *J. Phys.* **25,** 431 (1964).
17. H. BLANK AND C. RONCHI, *Acta Crystallogr. Sect. A* **24,** 657 (1968).
18. P. GANGULY AND C. N. R. RAO, *J. Solid State Chem.* **53,** 193 (1984).
19. R. D. SHANNON AND C. T. PREWITT, *Acta Crystallogr. Sect. A* **32,** 751 (1976).
20. A. F. WELLS, "Structural Inorganic Chemistry," Clarendon, Oxford (1984).
21. M. CRESPIN, P. LEVITZ, AND L. GATINEAU, *J. Chem. Soc. Faraday Trans. 2* **79,** 1181 (1983).
22. P. LACORRE, *J. Solid State Chem.* **97,** 495 (1992).
23. A. DEMOURGUES, J. C. GRENIER, A. WATTIAUX, J. P. DOUMERC, P. DORDOR, AND M. POUCHARD, to be published.
24. Y. TAKEDA, R. KANNO, M. SAKANO, O. YAMAMOTO, M. TAKANO, Y. BANDO, K. AKINAGA, K. TAKITA, AND J. B. GOODENOUGH, *Mater. Res. Bull.* **25,** 293 (1990).
25. K. K. SINGH, P. GANGULY, AND J. B. GOODENOUGH, *J. Solid State Chem.* **64,** 287 (1986).